

Decay and properties of the yrast superdeformed band in ^{192}Pb

D. P. McNabb,¹ J. A. Cizewski,¹ K. Y. Ding,¹ N. Fotiades,¹ D. E. Archer,² J. A. Becker,² L. A. Bernstein,² K. Hauschild,² W. Younes,² R. M. Clark,³ P. Fallon,³ I. Y. Lee,³ A. O. Macchiavelli,³ and R. W. MacLeod³

¹*Department of Physics and Astronomy, Rutgers University, New Brunswick, New Jersey 08903*

²*Lawrence Livermore National Laboratory, Livermore, California 94550*

³*Nuclear Science Division, Lawrence Berkeley National Laboratory, Berkeley, California 94720*

(Received 30 June 1997)

The $^{173}\text{Yb}(^{24}\text{Mg},5n)$ reaction at $E(^{24}\text{Mg}) = 134.5$ MeV with a gold-backed target was used to populate high-angular momentum states in ^{192}Pb . Resulting γ rays were detected with Gammasphere located at the 88-Inch Cyclotron. A discrete transition of energy $E_\gamma = 2057.7(6)$ keV has been identified in the depopulation of the yrast superdeformed (SD) band in ^{192}Pb . This transition has been tentatively placed in the level scheme based on coincidence relationships. Thus, the excitation energy of the SD level populated by the 262-keV in-band transition is tentatively assigned $E_x = 4.572(1)$ MeV. Confidence limits are discussed. Other transitions in coincidence with the SD band and general features of the band and its decay are also presented. In particular, we confirm that the $\mathcal{J}^{(2)}$ of the SD band decreases by $\approx 13\%$ at the lowest frequency. Also, by comparing the masses of the SD ground states in $^{192,194}\text{Pb}$ to liquid drop model expectations and to each other we have been able to confirm enhanced stability for $N = 112$ at superdeformation. [S0556-2813(97)02511-9]

PACS number(s): 21.10.Re, 23.20.Lv, 27.80.+w

I. INTRODUCTION

The excitation energies and spins of yrast superdeformed (SD) bands have recently been determined in ^{194}Pb [1–3], ^{194}Hg [4], and possibly ^{193}Pb [5]. These observations enable (1) the study of mechanisms involved in the decay of SD shapes, and (2) a test of the validity of microscopic static calculations which predict superdeformation, as for example in Krieger *et al.* [6]. In particular, the results presented here allow comparison between lead isotopes and test the prediction [6], for example, that the excitation energy of the SD bandhead in ^{192}Pb is lower than in ^{194}Pb . A more complete mapping of excitation energies, spins, and parities of SD levels will allow us to extract new information on the shell structure in the second well. In addition, a comparison of excitation energies in odd-even and even-even isotopes will enable us to extract information, albeit somewhat model dependent, on the pairing energy in the second well.

The SD band in ^{192}Pb has been observed previously in several experiments [7–9] and its isotopic assignment is well established. Previous spectroscopic work has been done in the first well for this nucleus and the work by Plompen *et al.* [10] and Van Duppen *et al.* [11] was used in the analysis presented here. The semimagic nature of lead isotopes, the expectation of a lower excitation energy for the second well in ^{192}Pb compared with ^{194}Pb , and the large amount of previous spectroscopic work available on this nucleus, makes ^{192}Pb an excellent candidate in which to search for primary γ -ray decay linking the SD states to yrast or near yrast states of normal deformation. From these linking transitions, the excitation energy and J^π of SD states can be established.

II. EXPERIMENTAL AND ANALYTIC PROCEDURES

The experiment was performed at the 88-Inch Cyclotron Facility at Lawrence Berkeley National Laboratory. The $^{173}\text{Yb}(^{24}\text{Mg},5n)$ reaction at a beam energy of 134.5 MeV

was used to populate high-angular momentum states in ^{192}Pb . The target was 1 mg/cm² of enriched ^{173}Yb evaporated on a 7-mg/cm² gold backing. The target was oriented at an angle of 27° to the beam. This reaction was chosen as it is qualitatively similar to the reactions successfully used in [1,3]. While it is a good choice for reducing the background due to fission, it does contain significant cross sections for other evaporation residues. The predominant exit channels were $^{191,192}\text{Pb}$ and ^{189}Hg , but ^{193}Pb , ^{190}Hg , and ^{191}Tl [12] were also populated. To reduce contamination from these evaporation channels, and events due to inelastic scattering, conditions on observed sum energy and multiplicity were set during the offline data analysis.

The γ -ray spectroscopy was done with the Gammasphere array, which consisted of 92 Compton-suppressed Ge detectors with Ta-Cu absorbers placed in front to reduce x rays and low-energy interactions in the detectors. The γ -ray pulse heights observed with the Ge detectors were recorded to tape with an analog-to-digital converter (ADC) resolution of about 3 ADC channels per keV. A total of 2.3×10^9 three-fold and higher coincidence events was collected. Time relationships were also recorded.

Relative photopeak efficiency and energy calibrations of the array over the range of 100–3548 keV were obtained in singles mode using standard ^{152}Eu , ^{182}Ta , and ^{56}Co sources. By comparing the intensities of the $5^- \rightarrow 4^+$ ($E1$) and $4^+ \rightarrow 2^+$ ($E2$) transitions [11] in ^{192}Pb , which are of similar energies, the relative detection efficiency of stretched dipole to stretched quadrupole transitions was determined to be 0.99(2). This is expected because of the large number of detectors in the array. Also, an energy-dependent, prompt time gate was used in the analysis. The time window was larger for lower-energy γ rays and the centroid also varied as a function of γ -ray energy to account for jitter and walk. By comparing the intensities of different lines in ^{192}Pb , we found no measurable change in the γ -ray intensities for $E_\gamma > 250$ keV in a time-gated spectrum. At about 125 keV,

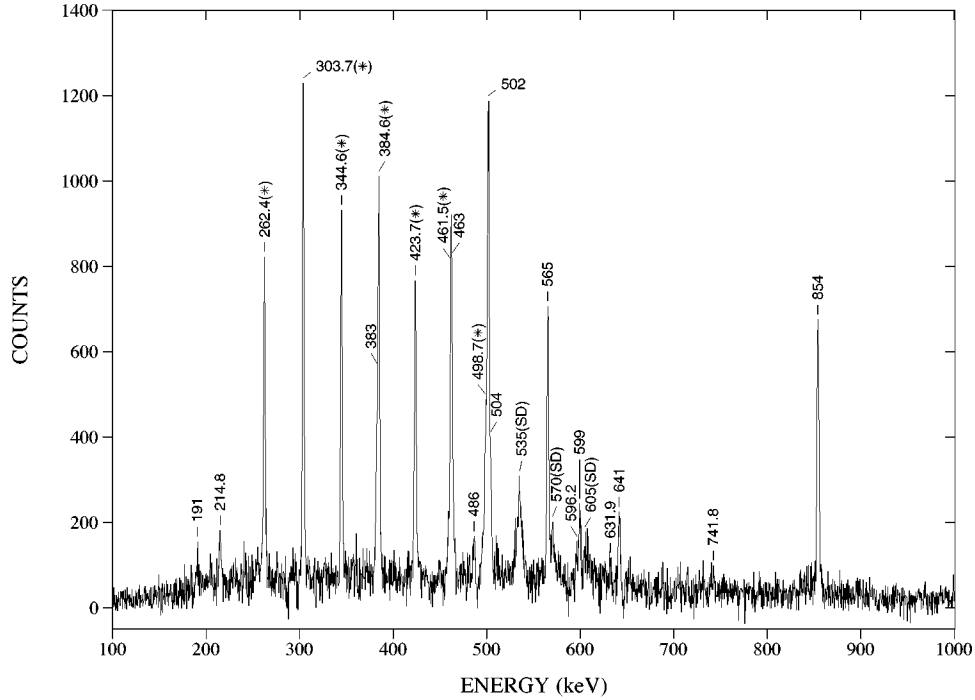


FIG. 1. Spectrum in ^{192}Pb sorted with the spike-free method [13] with the 13 different SD double-gate combinations discussed in the text. The band members marked with asterisks were used in the gating conditions. Dispersion is ≈ 0.33 keV/channel.

however, there is a marked reduction in the γ -ray intensity observed in a time-gated spectrum. No corrections to the γ -ray intensities were made to take into account either the effect of the prompt time gate or the angular distribution of the radiation.

The seven in-band SD transitions with energies from 262 to 499 keV were used as gating conditions when generating spectra in coincidence with the SD band. Double-gated events were sorted according to the spike-free method proposed by Beausang *et al.* [13]. Since the SD decay lines in ^{192}Pb were expected to be at energies close to the pairing energy, $2\Delta \sim 1.6$ MeV, there is particular reason to be concerned with contamination compared with the other successful linking experiments in the $A \sim 190$ region. Background subtraction was carried out in all three terms using the flat upper limit (FUL) method developed by Crowell *et al.* [14]. In addition, 10 of the 21 double-gate conditions, listed as (E_γ, E_γ) in keV, were excluded: the (262,304), (304,385), and (385,462) combinations, because of strong contamination from ^{190}Hg , and the (262,462), (262,499), (345,462), (345,499), (424,462), and (462,499) combinations, because of strong contamination from normal deformed states in ^{192}Pb , and the (304,462) combination because of background subtraction problems. The resultant spectra in two energy regions are shown in Figs. 1 and 2.

Corresponding to this spectrum, but not shown, is a spectrum of the variance for each channel. At each step in the data analysis, the variance spectrum was generated in accordance with the statistics of the experiment and background subtraction. This information was used to weight each channel when fitting peaks. Additional details of the analysis of spectra can be found in Sec. IV.

III. GENERAL FEATURES OF THE BAND AND ITS DECAY

The spectrum in Fig. 1 and individual double-gated spectra were analyzed in order to extract transition energies and a consistent set of intensities. The in-band energies and intensities are listed in Table I. The decay out of the SD band appears to occur at the four band members with lowest spin. Approximately 80% of the depopulation occurs at two of the SD levels. However, because there is only one transition with the maximum intensity, it is possible that the levels through which the band is fed and through which the decay out occurs are not exclusive of each other. Hence, the intensities cited in Table I and the text may be systematically too large. Also listed in Table I are the normal deformed transitions fed by the decay of the band. Since 69(5)% of the decay populates the 2_1^+ level and 3(1)% populates the 2_2^+ level, 28(4)% of the decay is not in prompt coincidence with the $2_1^+ \rightarrow 0_1^+$ or $2_2^+ \rightarrow 0_1^+$ transitions. The known isomeric levels in ^{192}Pb are $J^\pi = 10^+, 11^-, 12^+$, with half-lives of $T_{1/2} = 100(15)\text{ns}$, $95(15)\text{ns}$, $1.10(5)\mu\text{s}$ [12,15], respectively. Overall, the decay of the band appears to enter the previously known level scheme at levels with spins between $8 - 12\hbar$.

The γ ray at 1236.9(4) keV is in agreement with the $2_2^+ \rightarrow 0_1^+$ transition at $E_\gamma = 1237.7(3)$ keV previously observed in β^+ /electron capture decay [11]. This is consistent with the observation of the $2_2^+ \rightarrow 0_1^+$ transition in the ^{194}Pb SD decay experiment [3]. There is a line at 641 keV which we associate with the 641.5-keV line previously placed in the level scheme [10] as feeding the yrast 6^+ level, and not as an SD band member. If this were an SD transition, the line shape would be broadened in our data set because of the target backing and reaction kinematics, in contrast to the

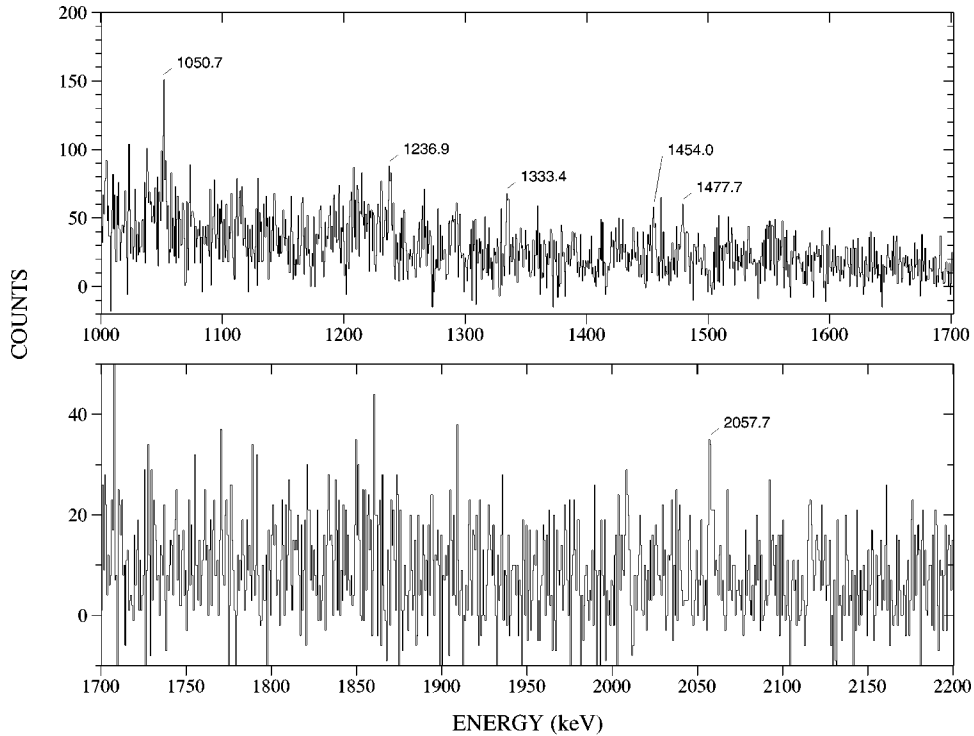


FIG. 2. Continuation of the spectrum displayed in Fig. 1. Dispersion is ≈ 0.66 keV/channel.

narrow line shape observed. In light of this, the candidate for an in-band SD transition at 640 keV as proposed in [8] should be reconsidered. Also, in [8], a line at 739.9 keV was observed and was assumed to be the $11^- \rightarrow 9^-$ transition [10]. In the present data set there is a weak line at 741.8(4) keV which is not consistent with our γ -ray energy of 739.6(1) keV for the $11^- \rightarrow 9^-$ transition, which we observed in an ND-gated spectrum. Instead, the 741.8(6)-keV γ ray has been placed as a transition which feeds the level depopulated by the 641-keV line just mentioned.

The existence of a 214.8(2)-keV transition proposed in [8] at the bottom of the band has been confirmed. This transition is interesting because the energy spacing between in-band transitions makes a significant upward change here. The energy spacing between the last two in-band transitions is 47.6(2) keV compared with 41.3(1) keV for the second and third transitions. This corresponds to a $\approx 13\%$ increase in $\mathcal{J}^{(2)}$, the dynamic moment of inertia, as a function of increasing rotational frequency. This has an important implication for the determination of the SD bandhead energy. Fitting the γ -ray energies to a rigid rotor with a first-order correction does not work well when including the new transition at 215 keV. Thus, the extrapolation to the bandhead excitation energy will only be reliable to within ~ 100 keV and care should be taken when drawing conclusions from such extrapolations. When the 215-keV γ ray is excluded, the fitted spin of the level populated by the 262-keV transition is $10.55(3)\hbar$, which is consistent with the previously calculated value [16].

IV. CANDIDATES FOR DISCRETE DECAY

The entire spectrum in Fig. 1 from 100 keV to 3 MeV was considered in the search for linking transitions. The high-

energy part of this spectrum is shown in Fig. 2. The spectrum was divided into 12 overlapping regions and each region was fitted with the GF2 program [17] using the variance spectrum discussed in Sec. II to weight the fit. All fits had $0.9 \leq \chi^2/\nu \leq 1.1$. For each fit, a pure Gaussian was assumed for the parent population of each γ ray, i.e., the ‘‘R’’ and ‘‘STEP’’ GF2 parameters were always fixed to zero. In addition, the width of each γ ray was fixed, except in the cases of the higher spin members of the SD band, which were expected to have broadened line shapes because of the backed target. The number of background channels always exceeded the number of peak channels. Hence, because the parameters used to fit the background have stable minima, we feel justified in assuming that the errors in the position and height of the peaks are accurately determined. For each peak we define a confidence parameter, $C = H/\Delta H$, where H is the height of the peak determined from the fit and ΔH its associated error. From these fits, we have listed in Table II fourteen previously unknown γ rays with $C \geq 3.8$. We chose 3.8σ as a cutoff point because the probability of observing a γ ray with $C \geq 3.8$ due to random background fluctuations is less than 50% for this value of C . This does not mean that peaks with $C < 3.8$ were not considered as linking transitions; rather we expect all peaks with $C \geq 3.8$ to be real, and must be understood.

Therefore, it is important to point out that Table II also contains two negative peaks. Our experience with the difficulties of background subtraction in multifold data is that these negative peaks represent the presence of systematic error in the background subtraction. Neither of these ‘‘ γ rays’’ shows any evidence of being in coincidence or anticoincidence with the band in spectra generated with a sum of double gates on the respective lines with the SD gating conditions. This type of systematic error in the background sub-

TABLE I. Gamma rays in ^{192}Pb deduced from the spectra displayed in Figs. 1 and 2. Intensities were derived from a spectrum obtained with clean double gates on the top γ rays in the band and normalized to the 345-keV SD-band transition. The intensities of higher-spin SD lines were derived from a double gate on the 304- and 345-keV transitions.

Transition (keV)	Placement ^a	Normalized intensity
214.8(2)	SD	0.05(2) ^b
262.4(1)	SD	0.45(3) ^b
303.7(1)	SD	0.87(3) ^b
344.6(1)	SD	1.00(4) ^b
384.6(1)	SD	0.85(7) ^b
423.7(2)	SD	0.67(6) ^b
461.5(2)	SD	0.31(4) ^b
498.7(2)	SD	0.27(5) ^b
191	$9^- \rightarrow 7^-$	0.16(4) ^c
383	$8^+ \rightarrow 6^+$	0.19(2) ^c
463	$7^- \rightarrow 5^-$	0.23(4) ^c
486	$9 \rightarrow 8^+$	0.06(2) ^d
502	$4^+ \rightarrow 2^+$	0.69(5) ^c
504	$5^- \rightarrow 4^+$	0.16(2) ^c
565	$6^+ \rightarrow 4^+$	0.49(4) ^c
596.2(4)		0.06(3) ^d
599	$8^+ \rightarrow 6^+$	0.13(3) ^d
631.9(4)		0.028(16) ^d
641	$2562 \rightarrow 6^+$	0.13(2) ^d
741.8(6)	$3304 \rightarrow 2562$	0.033(16) ^d
854	$2_1^+ \rightarrow 0^+$	0.69(5) ^c
1236.9(4)	$2_2^+ \rightarrow 0^+$	0.032(14) ^c
1333.4(5)		0.023(13) ^d
1477.7(6)		0.032(13) ^d
2057.7(6)	(SD $\rightarrow 9^-$)	0.041(12) ^d

^aTaken from [10] except when noted in the text.

^bCorrection due to electron conversion was estimated by calculation.

^cExperimentally measured [11] conversion coefficients were used.

^dNo correction for electron conversion was done for these intensities.

traction arises from oversubtraction or undersubtraction at energies that are particular to a given gating condition. It is very unlikely that such systematic errors will result in a false coincidence with the entire band.

From Table II, the new γ rays which are clearly in coincidence with the SD band in ^{192}Pb are 596.2(4)-, 631.9(4)-, 741.8(6)-, 1333.4(5)-, 1477.7(6)-, 2057.7(6)-keV lines. In some cases it was unclear whether or not a transition was in true coincidence with the band, because it was too close in energy to other lines in strong coincidence with the band. It is also possible that some of the other transitions included in Table II are shifted components of the SD transitions which have line shape due to the backed target. The placement of the 742-keV line was discussed in Sec. III. The placement of the 2057.7(6)-keV transition is discussed below. The 596.2(4)-, 631.9(4)-, 1333.4(5)-, and 1477.7(6)-keV lines have not been placed. The level scheme associated with the decay of the SD band in ^{192}Pb is displayed in Fig. 3.

The most likely candidate for a primary decay γ ray is the

highest energy candidate at 2057.7(6) keV. The coincidence spectrum of this line with the seven SD gates is shown in Fig. 4. The background subtraction for this spectrum was done in the same manner as discussed in Sec. II for Fig. 1. In addition, the smooth Compton and continuum background has been subtracted using the FUL method [14], modified for one-dimensional, background-subtracted spectra. While this spectrum is not visually exciting, we believe that the data conclusively indicate that the 2057.7(6)-keV transition is in coincidence with the SD band within at least a 99.97% confidence limit with respect to random statistical fluctuations. In support of this conclusion, we have two important arguments. First, as shown in Fig. 5, the relevant part of the spectrum in Fig. 4 is consistent with a Gaussian distributed set of channels with a mean of zero counts. This confirms that the background subtraction procedure and the propagation of errors was done correctly and also justifies our assumption that the confidence limit should be determined with respect to random statistical fluctuations. Second, the sum of counts for each SD transition is *not* consistent with zero counts with at least an 89% confidence limit for six of the seven transitions that were used for gating conditions. These counts are listed in Table III. Even if we assume that contaminant peaks are present in the spectrum and responsible for observation of the 2058-keV candidate link, the evidence for the 2058-keV link is still strong. For example, if the 345-keV and 385-keV transitions — the two lines with the most counts — are excluded, the sum of counts in the other five in-band transitions is *not* consistent with zero at a confidence level of 99.97%. The possibility that there is a broader structure in the neighborhood of 2058 keV which is responsible for the coincidence relationships in Table III has been ruled out. This was done by gating on the regions above and below the 2058-keV candidate in combination with the SD band. This failed to reproduce any evidence for coincidence with the SD band.

As can be seen from Table III, the data are consistent with the 214.8(2)-keV line being zero with a 66% confidence level. Conversely, the intensity of the 214.8(2)-keV line is not consistent with the expected value of 58(31) counts if the 214.8(2)-keV γ ray were part of the decay path which included the 2057.7(6)-keV transition. Hence, we have tentatively placed the 2057.7(6)-keV transition as depopulating the SD level which is fed by the 262.4(1)-keV in-band transition. We have also tentatively placed the 2057.7(6)-keV transition as decaying to the 9^- level at 2.514 MeV based on the data listed in Table III. We believe this to be the most likely placement based on these data. For example, all known γ rays which populate the 9^- level at 2.514 MeV are consistent with zero counts. We cannot rule out, however, that the 2057.7(6)-keV line is part of a multistep decay cascade, where the other transition(s) in the cascade is close in energy to a transition in Fig. 1.

Analysis of the other linking transitions was done in the same manner as with the 2058-keV line. These transitions have confidence limits of at least 99%. The γ rays at 1333.4(5) and 1477.7(6) keV are sufficiently high in energy to be considered candidates for primary decay. However, they show no evidence for being in coincidence with low-spin yrast transitions. These γ rays are, therefore, either decaying to structures built upon the 10^+ , 11^- , or 12^+ isomers

TABLE II. Transitions newly identified to be in coincidence with the SD band in ^{192}Pb . Lines present in the spectra of Figs. 1 and 2 are listed here if the confidence parameter $C \geq 3.8$. See text for further details.

Transition (keV)	C	Placement or comment
260.5(3)	5.87	Doublet with 262-keV line
425.9(4)	4.54	Doublet with 424-keV line
458.8(2)	9.43	Doublet with 461-keV line
465.3(3)	5.79	Doublet with 463-keV line
489.9(4)	-4.29	Negative peak
495.8(3)	7.99	Doublet with 499-keV line
596.2(4)	4.24	
631.9(4)	4.67	Similar energy to the $(\frac{29}{2}^+) \rightarrow (\frac{25}{2}^+)$ transition in ^{191}Pb [18]
645.8(4)	-3.82	Negative peak
741.8(6)	4.01	3304 \rightarrow 2562 keV
842.2(4)	3.94	Probably n, n' contaminant
856.4(4)	5.68	Doublet with 853-keV line
1050.7(4)	5.72	Contaminant from 424- and 345-keV gates
1236.9(4)	5.12	$2_2^+ \rightarrow 0_1^+$
1333.4(5)	3.95	
1477.7(6)	3.66	
2057.7(6)	4.54	(SD \rightarrow 9^-)

or involved in decay paths which bypass the yrast 2^+ state. For example, the excitation energies of the $J^\pi = 10^+, 11^-, 12^+$ isomers are 2581, 2743, and 2625 keV, respectively. A single transition between the same SD level depopulated by the 2058-keV transition and these isomers

would have energies of 1991, 1829, or 1947 keV, respectively, if the placement of the 2058-keV transition is correct. Hence, if the 1333- or 1478-keV lines feed an isomer then they must be decaying to a level which is part of a structure built upon that isomer.

At a γ -ray energy of 2 MeV we can place an upper limit on the intensity of unobserved linking transitions at $< 3.8\%$ for a peak with $C = 3.0$. The detection efficiency for events which decay to the $J^\pi = 10^+, 11^-, 12^+$ isomers is somewhat lower than events which decay to the ground state, because the multiplicity of such events is lower, and a software condition on multiplicity was used.

V. DISCUSSION

A. Excitation energy of the SD band in ^{192}Pb

We have tentatively placed the 2058-keV transition between the SD band member fed by the 262-keV transition and the 9^- yrast state at 2514 keV. This placement is based on the coincidence data discussed in the previous section. The tentative nature of this assignment is due to the minimal statistics in the current data set. As discussed above, this placement could be more definite if we had additional transitions which could be placed between the SD and ND levels to support the excitation energy assignment. However, the SD decay is observed to feed normal deformed levels of spin $8-12\hbar$, and the 9^- level, in particular, is observed to be fed by 16(4)% of the total decay. In the following we shall assume that this assignment is correct and the excitation energy of the SD state fed by the 262-keV transition is 4572(1) keV.

The placement of the 2058-keV transition between the SD band and the yrast 9^- state can be used to support a 10^+ spin-parity assignment for the initial SD state. There is every expectation that the yrast SD band in ^{192}Pb should have positive parity and even spin, because the yrast band in ^{194}Pb has

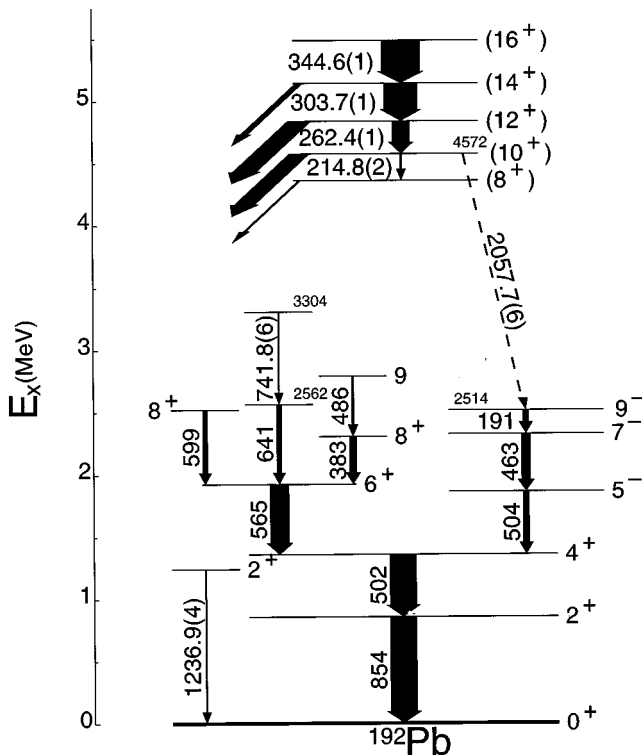


FIG. 3. The level scheme associated with the decay of the SD band in ^{192}Pb . The widths of the arrows are indicative of the intensities listed in Table I.

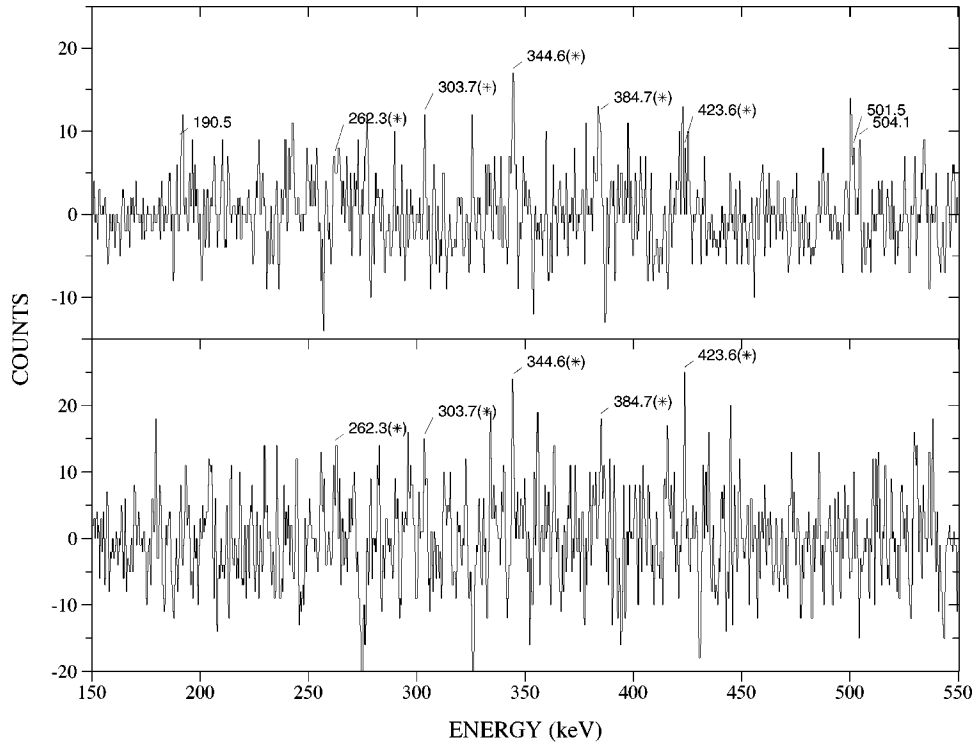


FIG. 4. (a) Spectrum in ^{192}Pb obtained from coincidence spectra with one gate on the 2057.7(6)-keV transition and the other taken from the set of seven SD gates between 262 and 499 keV. (b) Spectrum obtained with one gate on the 1333.4-keV transition and the other taken from the seven SD gating conditions. In order to guide the eye, the spectra have been smoothed over a range of three channels.

been measured experimentally [3] to have positive parity and because ^{192}Pb is even-even. Also, there is no known signature partner to the yrast SD band in ^{192}Pb , which argues that the band is built upon a $K=0$ bandhead. Our current understanding of the SD decay process is that SD states at the end of the known cascades have a small admixture of normal deformed states at high excitation energy [19]. It is likely that $\Delta L=1$ transitions will dominate [3,4] and the $E1$ strength function is typically larger than the $M1$ strength

function for normal deformed levels at high excitation energy. These arguments support a $J^\pi = 8^+$ or 10^+ value for the initial SD state. When combined with the level spin analysis discussed in Sec. III, a 10^+ value is preferred. Therefore, the 2058-keV transition is proposed to be a stretched $E1$ transition that connects the 10^+ SD level at $E_x = 4572(1)$ keV to the yrast 9^- state at 2514 keV.

Extrapolation to ascertain the (0^+) bandhead energy is difficult. As discussed in Sec. III, there is a dramatic increase

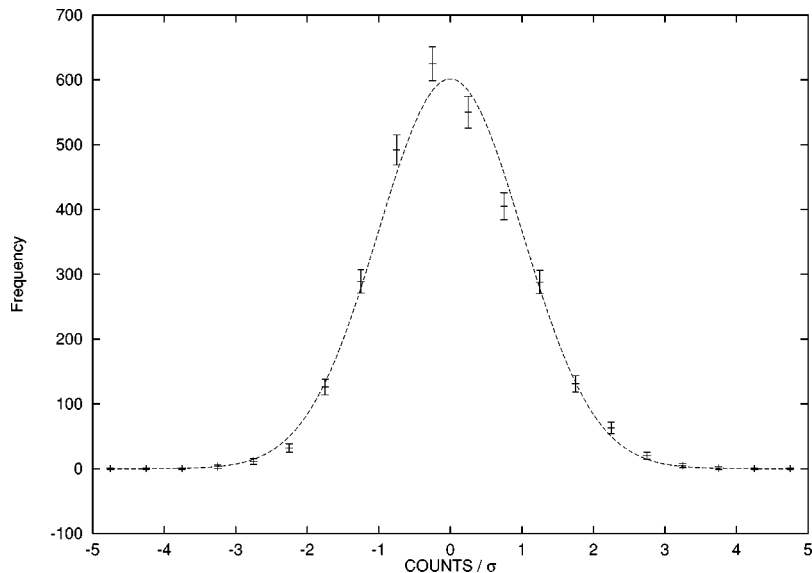


FIG. 5. The number of background-subtracted counts divided by the uncertainty σ calculated for that channel for each channel in the spectrum displayed in Fig. 4(a). The results are histogrammed in 0.5-unit wide bins. A Gaussian fit to the results is shown. For this fit, $\chi^2/\nu = 1.674$, $\sigma_{\text{fit}} = 1.007(9)$, and the mean, $\mu = 0.018(37)$.

TABLE III. Summary of γ -ray transitions associated with the spectrum shown in Fig. 4(a). The sum of counts over channels which were used as gating conditions is given; fits were not used because of low statistics. Intensities were corrected for K -shell electron conversion and normalized to the weighted mean of the intensities for each of the SD lines in the table, except for the 215-keV line. The higher spin SD transitions were normalized using the results in Table I before taking the weighted average. Further details are discussed in the text.

Transition (keV)	Placement	Sum of counts	Normalized intensity
215	SD	6(17)	0.10(29)
262	SD	45(18)	0.76(30)
304	SD	35(18)	0.60(31)
345	SD	86(19)	1.53(34)
385	SD	61(20)	1.13(37)
424	SD	39(19)	0.75(37)
462	SD	5(21)	0.10(42)
499	SD	37(23)	0.77(48)
191	$9^- \rightarrow 7^-$	38(20)	0.82(43)
463	$7^- \rightarrow 5^-$	-2(20)	-0.04(42)
502	$4^+ \rightarrow 2^+$	40(27)	0.86(58)
504	$5^- \rightarrow 4^+$	37(25)	0.79(54)
660	$10^{(-)} \rightarrow 9^-$	13(18)	0.32(44) ^a
740	$11^- \rightarrow 9^-$	-9(17)	-0.24(45)
854	$2^+ \rightarrow 0^+$	47(24)	1.35(70)

^aThis intensity has not been corrected for electron conversion because its multipolarity has not been assigned.

in $\mathcal{J}^{(2)}$ at the bottom of the SD band, where the γ -ray energy spacings are most sensitive to the spins of the levels. However, by excluding the 215-keV transition, we can estimate the excitation energy of the SD bandhead to be about 3.9 MeV. This is consistent with the expected isotopic trend predicted by calculations such as in [6], which predicted 4.00 MeV for the SD bandhead in ^{192}Pb . The calculations predict 4.86 MeV for the SD bandhead in ^{194}Pb , compared with the extrapolated value [3] of 4.6 MeV.

B. Microscopic contributions in SD Pb

The existence of a superdeformed minimum in the potential energy surface comes about from the competition between macroscopic and microscopic (shell) degrees of freedom. The shell effects can be highlighted by comparing the SD excitation energies in ^{194}Pb and ^{192}Pb . In the simple liquid drop model (LDM) the cold superdeformed 0^+ state can be modeled as a deformed liquid drop and a macroscopic comparison can be made between the difference in the normal ground-state and superdeformed ground-state masses. In the LDM, the addition of two neutrons, $(A, Z) \rightarrow (A+2, Z)$, increases the ground-state mass. However, the increase is expected to be larger in the superdeformed case compared to the spherical liquid drop because the surface-energy term provides the largest contribution to the change in binding energy for a deformed compared to a spherical shape. On the other hand, microscopic effects are responsible for the stability of the superdeformed shape, and hence microscopic effects should be sizable in the second well.

TABLE IV. Comparison between experimental and liquid-drop model calculations of mass differences for $^{192,193,194}\text{Pb}$ and ^{194}Hg . The LDM parameters used were $a_v = 15.56$, $a_s = 17.23$, $a_c = 0.697$, and $a_{\text{sym}} = 46.57$ MeV [20]. The normal ground-state masses and errors were taken from [21]. The errors quoted here also assume an error of 100 keV for the SD 0^+ bandheads. Energies and masses are given in MeV.

Nucleus	$E_{\text{exp}}^{\text{SD}} - E_{\text{LDM}}^{\text{SD}}$	$M_{\text{exp}}^{\text{ND}} - M_{\text{LDM}}^{\text{ND}}$	$M_{\text{exp}}^{\text{SD}} - M_{\text{LDM}}^{\text{SD}}$
^{194}Hg	-3.4(1)	-2.73(3)	-6.1(1)
^{194}Pb	-3.4(1)	-2.30(15)	-5.7(2)
^{192}Pb	-3.7(1)	-1.50(18)	-5.2(2)
^{193}Pb	-4.3(1)	-0.68(19)	-5.0(2)

In order to highlight such microscopic effects, differences between the masses extracted from experiment and calculated from the LDM, $M_{\text{exp}}^{\text{SD}} - M_{\text{LDM}}^{\text{SD}}$, are considered here for $^{192,193,194}\text{Pb}$ and ^{194}Hg . This quantity can be broken into two parts so that

$$M_{\text{exp}}^{\text{SD}} - M_{\text{LDM}}^{\text{SD}} = (E_{\text{exp}}^{\text{SD}} - E_{\text{LDM}}^{\text{SD}}) + (M_{\text{exp}}^{\text{ND}} - M_{\text{LDM}}^{\text{ND}}). \quad (1)$$

The macroscopic expression for the excitation energy of the superdeformed ground state in the LDM can be expressed to third order in the deformation parameter a_2 by [20]

$$E_{\text{LDM}}^{\text{SD}}(A, Z) = E_s \left[\frac{2}{5} (1-x)a_2^2 - \frac{4}{105} (1+2x)a_2^3 \right], \quad (2)$$

where x is the fissility parameter, $E_c/2E_s$, which is proportional to the ratio of the Coulomb energy (E_c) and surface energy at zero deformation (E_s) contributions to the LDM binding energy. We have also assumed the deformation parameter to be constant, $a_2 = 0.41$ ($\beta = 0.65$). The first term of Eq. (1) describes the macroscopic energy due to the deformation, and the second term accounts for a normal ground-state mass that differs from the LDM due to microscopic effects. The LDM predicts that $E_{\text{LDM}}^{\text{SD}}(^{192}\text{Pb}) = 7.63$ MeV, more than 3 MeV off from the empirical extrapolated value. The LDM model does a poor job at reproducing the magnitude of the excitation energy of the SD bandhead, because microscopic effects are important in this region of nuclei. However, the LDM does serve as a reference for macroscopic effects and that is exploited here. The LDM parameter values quoted in [20] and the evaluated ground-state masses from Audi and Wapstra [21] were used to determine $M_{\text{exp}}^{\text{SD}} - M_{\text{LDM}}^{\text{SD}}$. The results summarized in Table IV suggest that the superdeformed ground state in ^{194}Pb is slightly more bound — by 0.5(3) MeV — than in ^{192}Pb and, hence, the neutron number $N = 112$ is closer to a closed shell than $N = 110$. In addition, the result for ^{193}Pb may indicate that the pairing energy term is still present in the second well.

Hartree-Fock-Bogoliubov (HFB) calculations more closely reproduce the microscopic effects that lower the excitation energies of the SD bandheads in this mass region. However, there are still problems. In Table V the experimentally determined excitation energies are compared with two different HFB calculations. The axial HFB+BCS calculations using the Skm* effective interaction of Krieger *et al.* [6] are able to reproduce the data for the two lead isotopes,

TABLE V. Experimentally determined excitation energies in MeV compared with HFB calculations by Krieger *et al.* [6] and Girod *et al.* [22]. Empirical results are taken from [3,4] and the present work.

Nucleus	$E_x(\text{exp})$	$E_x(\text{Ref. [6]})$	$E_x(\text{Ref. [22]})$
^{194}Hg	6.0	5.00	6.49
^{194}Pb	4.6	4.86	4.55
^{192}Pb	(3.9)	4.00	3.61

but are 1 MeV too low for ^{194}Hg . A different approach by Girod *et al.* [22] uses the Gogny effective interaction, but calculates the zero-point energy through the solution of the Bohr Hamiltonian, which allows for nonaxial degrees of freedom and configuration mixing. These results are more satisfying, but are 0.5 MeV too high for ^{194}Hg , while only 0.3 MeV too low for ^{192}Pb .

C. Dynamical moments of inertia

In Fig. 6 we summarize the dynamical moments of inertia $\mathcal{J}^{(2)}$ for ^{192}Pb compared to ^{194}Pb . As noted in Sec. III, there is a 13% decrease in $\mathcal{J}^{(2)}$ at the bottom of the ^{192}Pb SD band. The only other case in the $A \sim 190$ SD region in which such a change in $\mathcal{J}^{(2)}$ at low frequency is observed is for the SD-4 band in ^{195}Pb , as displayed in Fig. 6. However, the decrease in $\mathcal{J}^{(2)}$ at the bottom of the ^{192}Pb SD band is considerably larger than observed in ^{195}Pb SD-4. In [23] the signature partner SD-3,4 bands are assigned as the $9/2^+$ [624] configuration. The SD band in the $N=110$ isotope ^{190}Hg has not been observed to sufficiently low frequency to allow a comparison with the $\mathcal{J}^{(2)}$ of ^{192}Pb at low frequency.

In the following discussion we will refer to the quasiparticle levels calculated in the cranked Woods-Saxon (CWS) approach of Wyss and co-workers [24]. In these calculations the $3/2^+$ [642], $3/2^-$ [761], $11/2^-$ [505], and $1/2^+$ [640] orbitals are just below the $N=112$ gap in the neutron single-

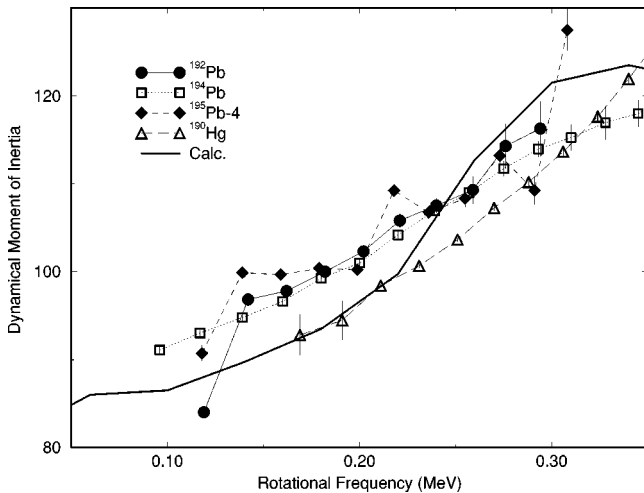


FIG. 6. Dynamical moments of inertia (in \hbar^2/MeV) for $^{192,194,195}\text{Pb}$ and ^{190}Hg as a function of rotational frequency. Data taken from [3,12,23] and the present work. Preliminary calculations from [25] are included.

particle levels and they are likely to play an important role near the Fermi surface in ^{192}Pb .

An increase in $\mathcal{J}^{(2)}$ as a function of increasing frequency can occur because of several factors. The most common reason is the alignment of particles with low Ω from orbitals with high angular momentum, such as the neutron $N=7$, $j_{15/2}$ intruder orbitals. However, such an explanation does not appear to be feasible in ^{192}Pb SD at low frequency. The main problem is that by spin $\approx 10\hbar$ the $\mathcal{J}^{(2)}$ of SD ^{192}Pb is essentially identical to that of SD ^{194}Pb . This would suggest that it is the alignment of particles near the Fermi surface at zero frequency that gives rise to this apparent upbend at $\hbar\omega \approx 100$ keV. The likely candidate for such an alignment could be the $3/2^-$ [751] orbital, which is at or slightly below the Fermi surface [24]. The data suggest that the alignment of this orbital needs to be complete by $\hbar\omega \approx 100$ keV to attain essentially identical moments of inertia above $\hbar\omega \approx 150$ keV between ^{194}Pb and ^{192}Pb . To further complicate this argument, the $\mathcal{J}^{(2)}$ in ^{194}Pb follows a smooth pattern down to the 6^+ SD state, or $\hbar\omega \approx 96$ keV, with no evidence for any upbend at low frequency. Another cause for a sudden increase in the $\mathcal{J}^{(2)}$ as a function of increasing frequency could be a sudden decrease in the pairing correlations. Again, the strong similarity in the $\mathcal{J}^{(2)}$ values of ^{192}Pb and ^{194}Pb above $\hbar\omega \approx 150$ keV suggests that the pairing correlations are rather similar. Since the increase in $\mathcal{J}^{(2)}$ observed in essentially all of the $A \approx 190$ SD bands is understood as arising from the gradual alignment of both neutrons and protons in intruder orbitals and a gradual decrease in the pairing correlations, it is unlikely that a sudden decrease at rather low frequencies in ^{192}Pb would not affect the pairing correlations at higher frequencies.

A third cause for a decrease in $\mathcal{J}^{(2)}$ at low frequency in SD ^{192}Pb could be a sudden decrease in the deformation. Near the Fermi surface is the oblate-driving $11/2^-$ [505] orbital [24]. It is possible that at the lowest frequencies the occupation of this orbital is favored, which also favors a lower deformation. To obtain a 13% decrease in $\mathcal{J}^{(2)}$ would require a decrease in deformation from $\beta=0.65 \rightarrow \beta=0.61$ for irrotational flow or $\beta=0.65 \rightarrow \beta=0.58$ for rigid body rotation. A measurement of the lifetimes of the levels at the end of the ^{192}Pb SD band would be a critical, albeit difficult, probe of the role of deformation in the dramatic change in the $\mathcal{J}^{(2)}$ at low spin.

A final cause for the decrease in $\mathcal{J}^{(2)}$ at the lowest spins observed in SD ^{192}Pb could be due to an accidental degeneracy with a ND state and an increased mixing with the ND levels. To obtain the ^{194}Pb pattern for the $\mathcal{J}^{(2)}$ values at the end of SD band in ^{192}Pb , the $10^+ \rightarrow 8^+$ SD transition should have an energy of about 220 keV, about 5 keV higher than observed. For the case of two-level mixing, the mixing matrix element between the SD and ND states could be as small as 5 keV, if the 8^+ SD level were exactly degenerate with an 8^+ ND state, to produce a 5 keV shift in the 8^+ SD level. However, such a value for this mixing matrix element is about two orders of magnitude larger than values extracted for the mixing between normal and SD levels at the end of the SD band in ^{194}Pb [26].

D. Implications for future SD→ND linking transition searches

The semimagic nature of ^{192}Pb and the lower excitation energy for the SD levels which decay to the normal levels

made ^{192}Pb a good candidate in which to search for linking transitions. In retrospect, given the limited statistics observed in candidates for discrete linking transitions in the present work, there are several difficulties which should be considered in future experiments proposed to search for discrete SD \rightarrow ND transitions in this mass region.

The most important result comes from the study of the quasicontinuum decay [27] of the SD bands in both ^{192}Pb and ^{194}Pb . These analyses suggest that the pairing-gap energy is smaller at spin $\approx 11\hbar$, the approximate spin at which the SD band in ^{192}Pb decays to ND states, compared with $\approx 7\hbar$, the approximate spin at which the yrast SD band in ^{194}Pb decays. This smaller pairing gap energy has two effects. First, it increases the phase space for multistep decay to the yrast line. Because the range of excitation energy between the pairing gap energy above yrast and the excitation energy of the SD band is increased, there is now a higher density of normal deformed levels through which the SD band can decay, and through which multistep paths can proceed. Second, the smaller pairing gap decreases the enhancement of primary decay over multistep decay which comes from the γ -ray energy factor in the transition probability [28].

The other important factor which complicated the present analysis is that ^{192}Pb is a more neutron-deficient system than ^{194}Pb . It is not possible to populate SD levels in ^{192}Pb as cleanly as can be attained in a heavier system, because there are more evaporation residue channels open in the more neutron-deficient compound system, as well as the increased cross section for fission. To search for discrete linking transitions, it is critical to have as many noncontaminated SD transitions as possible on which to select the SD cascade. This is especially important when the phase space for multistep processes is large because the pairing gap energy is small. Not only are contaminant lines themselves a problem, but also the background is increased from Compton-scattered and statistical γ rays present in a coincidence spectrum. In the present work there were many double-gate conditions that had to be rejected. Overall, the statistics for the SD band in this experiment are about 15% of the statistics collected for the linking experiment in ^{194}Pb reported in [3]. A more optimal reaction is one in which the evaporation residue of interest is well separated in γ -ray multiplicity from other evaporation residues, and fission is minimal.

VI. CONCLUSIONS

A single γ ray with an energy of 2057.7(6) keV has been tentatively placed as a transition linking the SD level populated by the in-band 262-keV transition to the 9^- level at an

excitation energy of 2514.2(5) keV. However, because of minimal statistics, we cannot rule out that the 2057.7(6)-keV line is part of a multistep decay cascade. We have argued that the spin of this SD level is most likely 10^+ if our placement of the linking transition is correct. The excitation energy of the 10^+ SD level is then 4.572(1) MeV and the bandhead excitation energy is estimated to be about 3.9 MeV. This result is consistent with the expectation [6] that the excitation energy of the yrast SD band at zero spin is lower in ^{192}Pb than ^{194}Pb . Four other previously unidentified γ rays of energies 596.2(4), 631.9(4), 1333.4(5), and 1477.7(6) keV have been shown to be in coincidence with the SD band, but have not been placed in the level scheme. Also, it has been shown that most of the decay of the band feeds previously known levels with spins of $8-12\hbar$ and that $\leq 28(4)\%$ of the decay feeds isomeric levels.

Given the deduced excitation energies of the SD bands in $^{192,194}\text{Pb}$, we have been able to extract the microscopic contributions to the SD masses. We have deduced that the microscopic contribution in SD ^{194}Pb is larger than in ^{192}Pb , which supports a larger shell gap at $N=112$ than at $N=110$ at large deformation, as expected from microscopic calculations, e.g., [24].

The $\mathcal{J}^{(2)}$ of the SD band in ^{192}Pb decreases by $\approx 13\%$ at the end of the band. It is possible that the decrease at low frequency is due to a decrease in deformation. Alternatively, it could represent the final transition in the alignment of the $3/2^-$ [751] configuration, although no similar alignment effects are observed at low frequency in ^{194}Pb .

It is unlikely in the near future that significant statistical improvements will be available to help identify transitions linking the SD band to normal levels in ^{192}Pb . A completely filled Gammasphere array, for example, will only improve statistics by about 30% for a similar 12-shift experiment. However, when an array such as Gammasphere is coupled to a recoil mass separator, such as the Fragment Mass Analyzer at Argonne, it is possible that the signal may be enhanced for discrete transitions which link the SD band to states which bypass isomers in the ND well by selection on the mass of the events.

ACKNOWLEDGMENTS

We would like to thank M. Girod for communicating results prior to publication and the staff of the 88-Inch Cyclotron for superb operation of the accelerator. This work has been funded in part by the National Science Foundation (Rutgers), the U.S. Department of Energy, under Contract Nos. W-7405-ENG-48 (LLNL), and AC03-76SF00098 (LBNL).

[1] M. J. Brinkman *et al.*, Phys. Rev. C **53**, R1461 (1996).
 [2] A. Lopez-Martens *et al.*, Phys. Lett. B **380**, 18 (1996).
 [3] K. Hauschild *et al.*, Phys. Rev. C **55**, 2819 (1997).
 [4] T. L. Khoo *et al.*, Phys. Rev. Lett. **76**, 1583 (1996).
 [5] S. Perries *et al.*, Z. Phys. A **356**, 1 (1996).
 [6] S. J. Krieger, P. Bonche, M. S. Weiss, J. Meyer, H. Flocard, and P. -H. Heenen, Nucl. Phys. A **542**, 43 (1992).

[7] E. A. Henry *et al.*, Z. Phys. A **338**, 469 (1991).
 [8] L. Ducroux *et al.*, Z. Phys. A **352**, 13 (1995).
 [9] S. J. Asztalos *et al.*, Z. Phys. A **352**, 239 (1995).
 [10] A. J. M. Plompen *et al.*, Nucl. Phys. A **562**, 61 (1993).
 [11] P. Van Duppen, E. Coenen, K. Deneffe, M. Huyse, and J. L. Wood, Phys. Rev. C **35**, 1861 (1987).
 [12] *Evaluated Nuclear Structure Data Files* (Brookhaven National

- Laboratory, Upton, NY, 1997).
- [13] C. W. Beausang, D. Prevost, M. H. Bergstrom, G. deFrance, B. Haas, J. C. Lisle, Ch. Theisen, J. Timar, P. J. Twin, and J. N. Wilson, Nucl. Instrum. Methods Phys. Res. A **364**, 560 (1996).
- [14] B. Crowell, M. P. Carpenter, R. G. Henry, R. V. F. Janssens, T. L. Khoo, T. Lauritsen, and D. Nisius, Nucl. Instrum. Methods Phys. Res. A **355**, 575 (1995).
- [15] J. M. Lagrange, M. Pautrat, J. S. Dionisio, Ch. Vieu, and J. Vanhorenbeeck, Nucl. Phys. **A530**, 437 (1991).
- [16] J. A. Becker *et al.*, Phys. Rev. C **46**, 889 (1992).
- [17] D. C. Radford, Program GF2 (unpublished).
- [18] N. Fotiades *et al.* (unpublished).
- [19] E. Vigezzi, R. A. Broglia, and T. Dossing, Nucl. Phys. **A520**, 179c (1990).
- [20] S. G. Nilsson and I. Ragnarsson, *Shapes and Shells in Nuclear Structure* (Cambridge University Press, Cambridge, England, 1995), Chap. 4.
- [21] G. Audi and A. H. Wapstra, Nucl. Phys. **A565**, 1 (1993).
- [22] M. Girod (private communication).
- [23] L. P. Farris *et al.*, Phys. Rev. C **51**, R2288 (1995).
- [24] R. Wyss, W. Satula, W. Nazarewicz, and A. Johnson, Nucl. Phys. **A511**, 324 (1990).
- [25] P. Fallon (private communication).
- [26] R. Krucken *et al.*, Phys. Rev. C **55**, R1625 (1997).
- [27] D. P. McNabb *et al.*, Bull. Am. Phys. Soc. **41**, 1237 (1996); (unpublished).
- [28] A. deShalit and H. Feshbach, *Theoretical Nuclear Physics Vol.1: Nuclear Structure* (Wiley, New York, 1974), p. 698.